Available online at www.ijpe-online.com

International Journal of Performability Engineering

vol. 15, no. 5, May 2019, pp. 1400-1407
DOI: 10.23940/ijpe.19.05.p16.14001407

Lubrication Characteristics Analysis of a Rotor Bearing for Space Application

Shouqing Huang, Shouwen Liu*, Xiaokai Huang, and Fangyong Li

Beijing Key Laboratory of Environment and Reliability Test Technology for Aerospace Mechanical and Electrical Products Beijing Institute of Spacecraft Environment Engineering, Beijing, 100094, China

Abstract

Concerning the problem of lubrication failure of high speed rotor bearings, a unified model of mixed lubrication is built for angular contact ball bearings with comprehensive consideration of the effects of contact geometry, real rough surface topography, elastic deformation, rheological properties of lubricants, high speed spinning properties of balls, and other factors. On this basis, the effect laws of rotate speed, load, vacuum, high and low temperature, and other working and environmental conditions on the contact and lubrication properties of the microscopic transmission interface of a bearing are analyzed, laying a theoretical basis for the application of high speed rotor bearings in a multi-stress space environment.

Keywords: high speed rotor bearing; multi-stress; mixed lubrication numerical analysis

(Submitted on December 12, 2018; Revised on January 15, 2019; Accepted on February 17, 2019)

1. Introduction

High speed rotor bearing is a core element of gyroscopes, momentum wheels, or any other spatial moving part, and its precision, service life, and reliability have great effects on the service performance of such spatial moving parts [1]. The development of highly swift and quick maneuverable aircraft technology is increasingly demanding on spatial high speed rotor bearings. According to the statistical analysis of in-orbit faults of satellites [2-3], over 50% of attitude and orbit control system faults result from gyroscopes, momentum wheels, and other spatial moving parts, wherein lubrication faults of bearings occupy a higher ratio [4].

Concerning the kinematical and stress analysis of rolling bearings, Jones [5] was the first to build a quasi-static analysis model of ball bearings and apply such a model to studying issues of static kinematics and mechanics. On the basis of Jones's work, Harris [6] put forward a computational method of quasi-dynamics and set up a balanced nonlinear equation set of rolling element, cage, and inner ring to analyze the revolution and autorotation speed of the rolling element, bearing deformation, etc. Gupta [7] built a dynamic analysis model for rolling bearings to compute the displacement and rotate speed of ball and cage at any moment after a bearing rotates and slides in the bearing. Concerning the effects of surface topography on lubrication performance, Ai and Cheng [8-9] firstly studied the effects of single pit and rough surfaces of different texture directions on elasto-hydrodynamic lubrication performance by a deterministic model. Later, Xu and Sadeghi [10] and Zhu and Ai [11] further studied the elasto-hydrodynamic lubrication performance of the measured rough surface. Such studies were in the scope of full-film elasto-hydrodynamic lubrication in spite of their consideration of surface roughness. Subsequently, Jiang et al. [12], Hu and Zhu [13], as well as Holmes et al. [14] presented different deterministic mixed lubrication models in succession. Zhu and Hu [15] studied the effects of different rough surface topography and surface roughness on mixed lubrication performance by a unified Reynolds equation. Sahlin et al. [16-17] performed a simulated computation and experimental verification on the mixed lubrication model in consideration of real three-dimensional rough surfaces. Few of the studies above were concerned with effects of vacuum, microgravity, high and low temperature, and other typical space environments on lubrication properties.

* Corresponding author.
E-mail address: 2316879635@qq.com

Concerning the above problems, it is planned to study effects of rotate speed, load, vacuum, high and low temperature, and other working conditions and environmental conditions on microscopic transmission interface contact and lubrication properties of a bearing by a mixed lubrication model in consideration of rough surface topography in this paper.

2. Kinematical Analysis on a Bearing

The inner and outer rings of a rolling bearing generally generate simpler motion, which generally generates fixed-axis rotation. The rolling element has a more complicated state of motion, which leads to revolution around the axis of the bearing and autorotation around its own axis. In a high speed bearing whose contact angle is higher than zero, the relative ball track of the rolling element causes autorotation around the normal line of the point of contact.

Without regard to the autorotation of the ball, the revolution speed n_m and angular speed of autorotation n_b of the ball are computed respectively as follows:

$$n_m = \frac{1}{2}[n_i(1-\gamma) \mp n_e(1+\gamma)] \tag{1}$$

$$n_b = \frac{d_m}{2D_w}(n_i \pm n_e)(1-\gamma^2) \tag{2}$$

In the equation, n_i, n_e are the rotate speed of fixed-axis rotation of the inner ring outer ring of the bearing, respectively; d_m is the pitch diameter of the bearing and $d_m = (d_i + d_e)/2$, where d_i, d_e refer to the diameter of the ball track of the inner ring and outer ring, respectively; D_w is the diameter of the steel ball; and γ is the intermediate coefficient, where $\gamma = D_w\cos\alpha/d_m$. If the inner and outer rings rotate in the opposite direction, the symbol above shall be valued; if the inner and outer rings rotate in the same direction, the symbol below shall be valued.

Computing results under actual working conditions (assuming that the outer ring is fixed and the inner ring is in the rotate speed of n_i): the change of the contact angle resulting from load bearing, revolution, and autorotation speed of the bearing ball under different working conditions of rotate speed can be drawn by computation.

3. Mixed Lubrication Numerical Analysis and Control Equation of a Bearing

A mixed lubrication model in consideration of macroscopic contact geometry, real microscopic rough surface topography, high speed autorotation properties, elastic deformation, and rheological properties of lubricants is built to compute contact and lubrication properties between the ball and inner and outer ball track transmission interface under different working conditions (rotate speed, temperature, and load), generally including: film thickness, ratio of contact area of micro asperities on the rough surface, and maximum pressure in the contact area. The oil starvation at the inlet of the lubricant resulting from the centrifugal force and microgravity is equalized by decreasing the inlet film thickness.

The pressure in the whole solution domain is controlled by Reynolds equation. Assuming that the x axis is in the same direction as the rotation direction, the equation is as follows:

$$\frac{\partial}{\partial x}\left(\frac{\rho h^3}{12\eta}\frac{\partial p}{\partial x}\right) + \frac{\partial}{\partial y}\left(\frac{\rho h^3}{12\eta}\frac{\partial p}{\partial y}\right) = u\frac{\partial(\rho h)}{\partial x} + \upsilon\frac{\partial(\rho h)}{\partial y} + \frac{\partial(\rho h)}{\partial t} \tag{3}$$

In the equation, p is the pressure distributed in the solution domain; h is the film thickness; u is the speed in the x direction; υ is the speed in the y direction; and η is the lubricant viscosity, related to pressure. The common equation is a viscosity equation in line with the index law:

$$\eta = \eta_0 e^{\alpha p} \tag{4}$$

Where ρ is the lubricant density, which is a function of pressure generally computed in the following equation:

$$\rho = \rho_0 \left(1 + \frac{0.6 \times 10^{-9} p}{1 + 1.7 \times 10^{-9} p} \right) \tag{5}$$

In consideration of the non-Newtonian fluid behavior of lubricant, the effective viscosity η^* is calculated as follows [18]:

$$\frac{1}{\eta^*} = \frac{1}{\eta} \frac{\tau_0}{\tau_1} \sinh\left(\frac{\tau_1}{\tau_0} \right) \tag{6}$$

In the equation, η is the viscosity under low shear strain rate, τ_1 is the shear stress applied on the lower surface, and τ_0 is the reference shear stress.

In terms of point contact, the local film thickness/clearance depends upon time, which may be expressed in the following equation [19]:

$$h = h_0(t) + \frac{x^2}{2R_x} + \frac{y^2}{2R_y} + v_e(x, y, t) + \delta_1(x, y, t) + \delta_2(x, y, t) \tag{7}$$

Where $h_0(t)$ refers to the film thickness in the center of the rigid body, $\frac{x^2}{2R_x} + \frac{y^2}{2R_y}$ refers to the original macroscopic geometric contact, v_e refers to the elastic deformation on the surface resulting from the distributed pressure, and δ_1, δ_2 refer to three-dimensional original roughness of the contact surface.

The elastic deformation on the surface is computed by the Boussinesq integral in the following formula:

$$v_e(x, y, t) = \frac{2}{\pi E'} \iint_\Omega \frac{p(\xi, \zeta, t)}{\sqrt{(x - \xi)^2 + (y - \zeta)^2}} \mathrm{d}\xi \mathrm{d}\zeta \tag{8}$$

In the state of mixed lubrication, the load is borne by film and contact of micro asperities on the rough surface, and the applied load is balanced by the distributed pressure. Therefore, it can be solved by solving the integral of pressure in the whole solution domain:

$$w(t) = P_c + P_f = \sum_{i=1}^{N} \iint_{A_{ci}} p_{ci} \mathrm{d}A_{ci} + \iint_\Omega p(x, y, t) \mathrm{d}x \mathrm{d}y \tag{9}$$

In the equation, P_f is the normal load borne by film, P_c is the normal load borne by asperities, p_{ci} is the contact pressure of single asperity, A_{ci} is the contact area of single asperity, and i is the contact number of asperities.

In the state of mixed lubrication, there are the following major evaluation indexes: the film thickness ratio λ is the ratio of the mean of the film thickness and the compound root mean square (RMS) of roughness in the half contact width, the ratio of the contact area of the rough surface A_c is the ratio of the contact area of the rough surface and the Hertz contact area, and ratio of the contact load of the rough surface W_c is the ratio of the contact load of the rough surface and the total contact load.

In Equations (3) to (9), elastic deformation, viscosity, and density of the lubricating oil are functions of pressure, which are combined with the Reynolds equation to an integral differential equation set solved by the quasi system method [20], where the item of elastic deformation is computed by FFT. The pressure of each node discretizes the integral differential equation set to be a difference equation to make discretization of the two items on the left of the Reynolds equation by second order central difference, make backward difference by first order, complete discretization of the two items on the right of the equation, and make matrix conversion of pressure and influence coefficient to the frequency domain to greatly decrease the computed amount. The Hertz pressure distribution is regarded as the initial pressure distribution to estimate the

initial value of elastic deformation. The original clearance is substituted into the film thickness equation to compute the initial film thickness and substituted into the Reynolds equation to solve the pressure of all nodes and update the film and deformation by such pressure. The pressure distribution, film thickness, and elastic deformation are computed in a repetitive way by Gauss-Siedel iteration until the pressure and load conversion precision are met (0.000001). In the iteration, the solution domain of the Reynolds equation is $-3 \le Y \le 3$. In the whole solution domain, the computational grid is 257×257, the pressure convergence precision is $\varepsilon_p = \Sigma \left| P_{i,j}^{new} - P_{i,j}^{old} \right| / \Sigma P_{i,j}^{new} < 0.00001 \sim 0.0001$, and the load convergence precision is $\varepsilon_w = \left| w^{new} - w^{old} \right| / w^{new} < 0.00001 \sim 0.0001$.

4. Results of Mixed Lubrication Numerical Analysis of a Bearing

A typical 7304 angular contact ball bearing is taken as target in the analysis in which all input parameters and conditions are as follows: the contact angle is 15o, the bearing rings and ball are made of 9Cr18Mo, the inner diameter and outer diameter of the bearing are 20mm and 47mm respectively, the diameter of the ball is 6.5mm, and the radius of curvature of the channels of the inner and outer rings is 3.58mm. The surface roughness of the channels is about Ra0.032, and the surface roughness of the ball is about Ra0.016. The bonding pressure index of the lubricating oil applied is $2.2 \times 10^{-8} m^2/N$, the viscosity of the lubricating oil is $60 mm^2/s$ in 20℃, the viscosity of the lubricating oil is $9.560 mm^2/s$ in 100℃, and the density of the lubricating oil is $1.87 g/cm^3$. The results of mixed lubrication numerical analysis on the bearing are as follows.

According to the analysis results in Figures 1 and 2, as the rotate speed of the bearing gradually rises from 0.01r/min to 16000r/min, the proportional range of the contact area of rough peak micro asperities in the contact interface is 0%-100% (as shown in Figure 2(b)), and the lubrication state has covered the full-film, mixed, and boundary lubrications. The critical rotate speed for conversion from the boundary lubrication to the mixed lubrication is around 20r/min and that for conversion from the mixed lubrication to the elasto-hydrodynamic lubrication is around 800r/min.

As shown in Figure 1(a), when the rotate speed is 0.01r/min, the pressure peak of interface is 2.6GPa at the maximum. The pressure peak of the interface decreases as the rotate speed rises. When the rotate speed is 16000r/min, the pressure peak is 1.3078GPa at the minimum. This is mainly because when the bearing is at a low speed, it is in the state between boundary and mixed lubrication, the ratio of the contact area and load borne by micro asperities is larger, and micro asperities on the rough surface contact and embed each other to create high viscosity and pressure films in local areas. However, as the rotate speed rises, the film thickness gradually rises, the load approaches equilibrium, and the situation is improved.

According to results of kinematical analysis on the bearing, when the bearing is at the input rotate speed of 16000r/min, the spin speed of the steel ball attains 465.6r/min. Since the radius of curvature of the contact area in the spin direction is only 0.2mm, the spin speed is converted to a lower linear speed. As a result, it does not have obvious effects on the lubrication state.

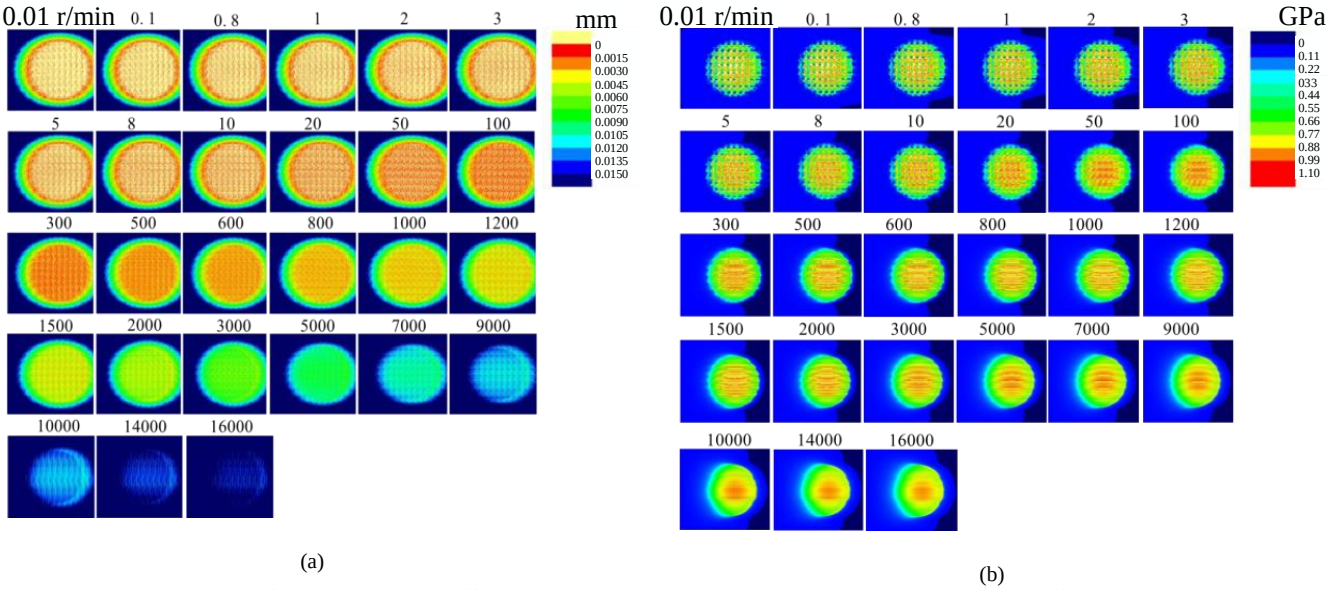

(a) (b)

Figure 1. (a) Distributions of film thickness under different rotate speed conditions; (b) Distributions of pressure under different rotate speed conditions

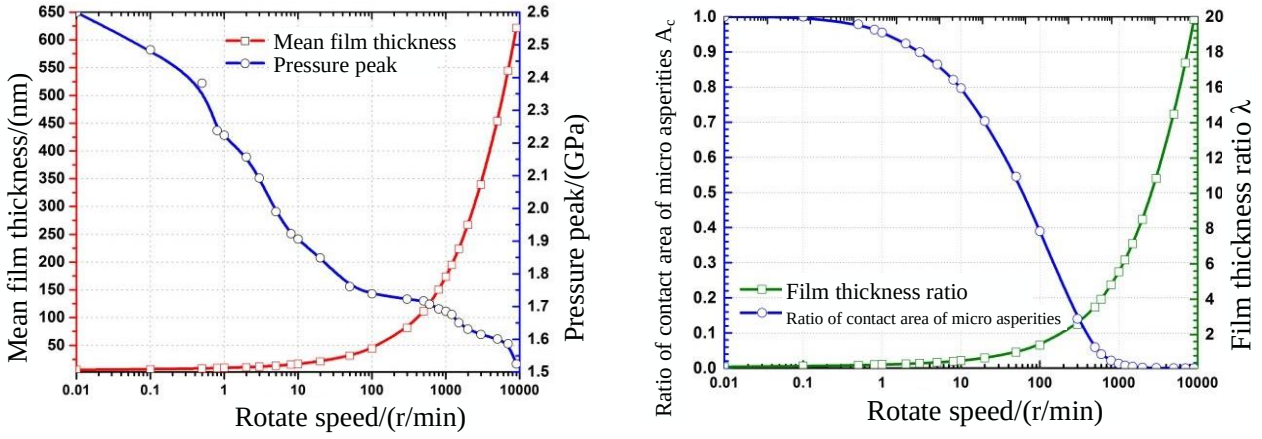

(a) (b)

Figure 2. (a) Film thickness and pressure peak height; (b) Film thickness ratio and contact area ratio under different rotate speed conditions

According to analysis results in Figure 3, four load levels have minor effects on film thickness mainly because in the state of mixed lubrication, the film stiffness is much higher than that of micro asperities, and the load rise increases the film pressure but has minor effects on the contact degree of micro asperities and film thickness. Therefore, the increased load is generally borne by film thickness, whereas the load has remarkable effects on the pressure peak of the interface in the contact area of the bearing, and the pressure peak of the interface rises as the load rises as a whole. However, when the bearing is at an extremely low rotate speed (lower than 0.5r/min), the pressure peak of the interface in the load of 80N is lower than that in the load of 70N, 60N, and 35N. This is mainly because the load has some flattening effects on the topography of the rough surface to decrease the contact stress between micro asperities; as the rotate speed rises, the regularity in which the pressure peak of interface increases as the load increases becomes better.

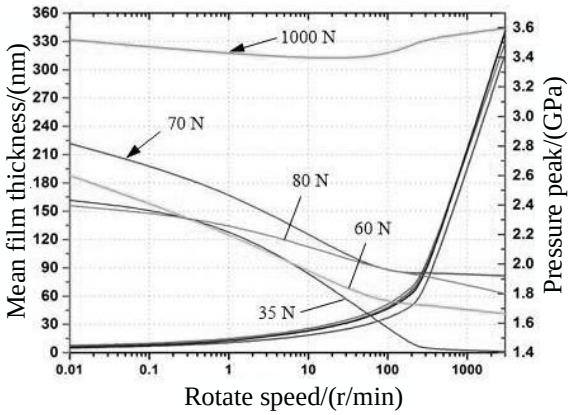

Figure 3. Effects of load on film thickness and interface pressure (20℃)

According to Equations (5) and (6) for describing rheological properties of a lubricant, the atmospheric pressure generally changes lubrication properties by influencing the viscosity and density of the lubricating oil. Therefore, the film thickness increases while the pressure peak of the interface decreases as the atmospheric pressure increases (as shown in Figure 4). As the atmospheric pressure is in the exponential relationship with both viscosity and density of the lubricating oil, the viscosity and density change only slightly as the pressure changes in the vacuum environment of extremely low pressure. As a result, the pressure does not have obvious effects on the lubrication state of the bearing.

According to analysis results shown in Figure 5(a), as the temperature rises, the viscosity of the lubricating oil decreases and thereupon the film thickness decreases. As the rotate speed rises, the temperature shows more remarkable effects on the film thickness. The pressure peak of the interface increases as the film thickness decreases. Since the decrease in film thickness may remarkably increase the area of direct contact of micro asperities and the load borne in the interval of boundary and mixed lubrication (0.01r/min~200 r/min), the increase in pressure peak of the interface is clearer in this interval. In addition, as the rotate speed rises, the contact interface enters the elasto-hydrodynamic lubrication interval, which is gradually separated by the film. As a result, the effects of temperature on the interface pressure gradually weaken (as shown in Figure 5(b)).

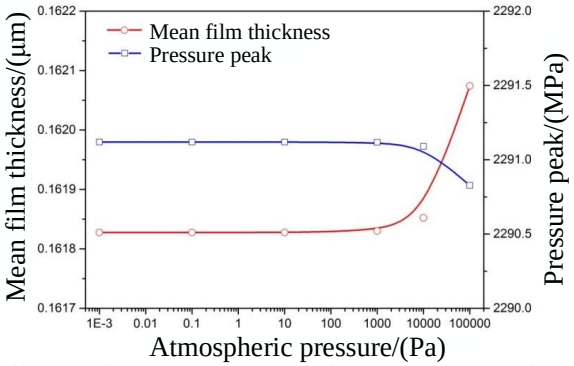

Figure 4. Effect law of atmospheric pressure on film thickness and interface pressure

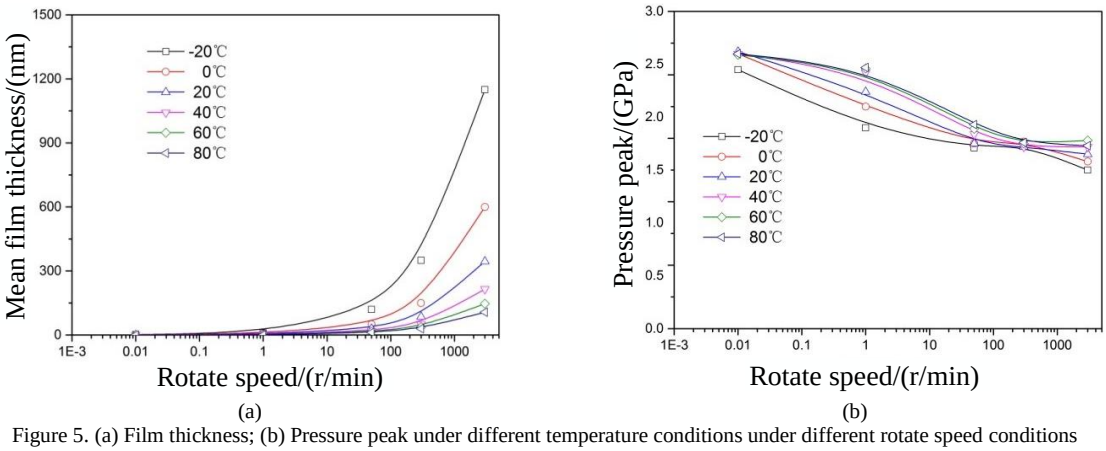

(a) (b)

Figure 5. (a) Film thickness; (b) Pressure peak under different temperature conditions under different rotate speed conditions

The centrifugal force and microgravity lead to oil starvation at the inlet of the lubricant and reduce film thickness of the lubricating oil primarily by influencing the supply of the lubricant. In order to analyze the effects of oil starvation on the lubrication state of a bearing under different rotate speed conditions, three rotate speed conditions including 200r/min, 1000r/min, and 3000r/min under the load condition of 70N are set for comparative analysis. At the inlet of the contact area, seven different groups of inlet film thickness are set to simulate states of oil starvation at different degrees. The lower the inlet film thickness is, the greater degree the oil starvation shall be.

According to analysis results in Figure 6, the mean film thickness in the contact area increases as the inlet film thickness increases. Under the low speed condition, as the inlet lubricating oil does not have obvious entrainment effects, the contact area is in the boundary or mixed lubrication state, the initial value of film thickness is lower, and the oil starvation at the inlet does not have obvious effects on the film thickness.

As the rotate speed rises, the entrainment effects of the inlet lubricating oil increase while the supply of the lubricant has great effects on the film thickness. Under the high speed condition, this phenomenon becomes clearer, and the mean film thickness in the state of oil starvation declines by about 44% compared to when it is in the state of sound lubrication. Thus, it is sufficient to change the lubrication state of the transmission interface of a bearing.

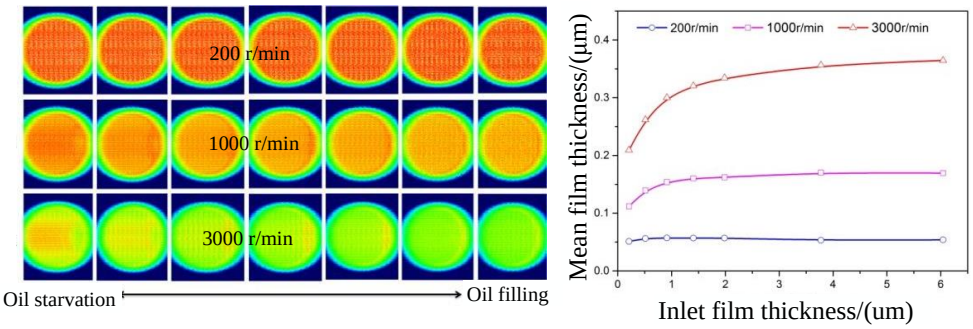

Figure 6. Effect law of oil starvation on film thickness under different rotate speed conditions

5. Conclusions

The mixed lubrication numerical analysis is made on the 7304 angular contact ball bearing in which effects of macroscopic contact geometry, real microscopic rough surface topography, high speed spinning properties, elastic deformation, rheological properties of the lubricant, and other factors are comprehensively taken into account and a unified model of mixed lubrication analysis on angular contact bearings is built. On this basis, effect laws of rotate speed, load, vacuum, high and low temperature, and other working and environmental conditions on microscopic transmission interface contact and lubrication properties of bearings are studied, laying a theoretical basis for the application of high speed rotor bearings in a multi-stress space environment. The major conclusions are as follows:

1) As the rotate speed rises, the lubrication state of the contact interface of a bearing is gradually improved, the critical rotate speed for conversion from the boundary lubrication to the mixed lubrication is around 20r/min, and that for the conversion from the mixed lubrication to the elasto-hydrodynamic lubrication is around 800r/min. In the range of rotate speed of 0-16000r/min, the spinning of the steel ball does not have obvious effects on the lubrication state.

2) The pressure peak of the contact interface of a bearing increases as the load rises as a whole. At an extremely low rotate speed (lower than 0.5r/min), the load has minor effects on film thickness because the load has some flattening effects on the topography of the rough surface and load increase within some limit facilitates stress concentration in contact of micro asperities.

3) As the atmospheric pressure increases, the film thickness increases while the pressure peak of interface decreases. However, such effects are not remarkable. The film thickness decreases as the temperature increases and as the rotate speed rises, the temperature has clearer effects on the film thickness. The interface pressure increases as the temperature rises, and such effects become clearer in the area of boundary and mixed lubrication only.

4) Under the low speed condition, the inlet oil starvation caused by the centrifugal force and microgravity has minor effects on lubrication properties. As the rotate speed rises, the entrainment effects of the inlet lubricating oil increase while the supply of the lubricating oil has greater effects on the film thickness.

Acknowledgements

This research was support by the Equipment Development Department of PLA (No. 41402010103).

References

1. C. He and D. Li, "Research on Reliability of Gyro Motors," *Aerospace Control* (*in Chinese*), pp. 74-81, 2002
2. S. Zhang, J. Shi, and J. Wang, "Satellite on-Board Failure Statistics and Analysis," *Spacecraft Engineering* (*in Chinese*), Vol. 19, No. 8, pp. 41-46, 2010
3. R. R. Burt, R. W. Loffi, and T. B. Company, "Failure Analysis of International Space Station Control Moment Gyro," in *Proceedings of the 10th European Space Mechanisms & Tribology Symposium*, pp. 13-25, San Sebastian, Spain, September 2003
4. K. Sathyan, K. Gopinath, S. H. Lee, and H. Y. Hsu, "Bearing Retainer Designs and Retainer Instability Failures in Spacecraft Moving Mechanical Systems," *Tribology Transactions*, Vol. 55, No. 4, pp. 503-511, 2015
5. A. B. Jones, "Ball Motion and Sliding Friction in Ball Bearings," *Journal of Basic Engineering*, 1959
6. T. A. Harris and M. N. Kotzalas, "Rolling Bearing Analysis: Advanced Concepts of Bearing Technology," 5th Edition, CRC Press, Boca Raton, 2006
7. P. K. Gupta, "Advanced Dynamics of Rolling Elements," Springer, Vienna, 1984
8. X. Ai and H. Cheng, "The Effects of Surface Texture on EHL Point Contacts," *Journal of Tribology*, Vol. 118, No. 1, pp. 59-66, 2008
9. X. Ai and H. Cheng, "The Influence of Moving Dent on Point EHL Contacts," *Tribology Transactions*, Vol. 37, No. 2, pp. 323-335, 2008
10. G. Xu and F. Sadeghi, "Thermal EHL Analysis of Circular Contacts with Measured Surface Roughness," *Journal of Tribology*, Vol. 118, No. 3, pp. 473-482, 2008
11. D. Zhu and X. Ai, "Point Contact EHL based on Optically Measured Three-Dimensional Rough Surfaces," *Journal of Tribology*, Vol. 119, No. 3, pp. 375-384, 2008
12. X. F. Jiang, D. Y. Hua, H. S. Cheng, X. L. Ai, and S. C. Lee, "A Mixed Elastohydrodynamic Lubrication Model with Asperity Contact," *Journal of Tribology*, Vol. 121, No. 3, pp. 481-491, 2008
13. Y. Z. Hu and D. Zhu, "A Full Numerical Solution to the Mixed Lubrication in Point Contacts," *Journal of Tribology*, Vol. 122, No. 1, pp. 1-9, 2008
14. M. J. A. Holmes, H. P. Evans, T. G. Hughes, and R. W. Snidle, "Transient Elastohydrodynamic Point Contact Analysis using a

New Coupled Differential Deflection Method Part 1: Theory and Validation," in *Proceedings of the Institution of Mechanical Engineers*, pp. 333-365, 2003
15. D. Zhu, "Effect of Surface Roughness on Mixed EHD Lubrication Characteristics," *Tribology Transactions*, Vol. 46, No. 1, pp. 44-48, 2008
16. F. Sahlin, R. Larsson, A. Almqvist, P. Lugt, and P. Marklund, "A Mixed Lubrication Model Incorporating Measured Surface Topography, Part 1: Theory of Flow Factor," *ARCHIVE Proceedings of the Institution of Mechanical Engineers Part J Journal of Engineering Tribology*, DOI: 10.1243/13506501JET658, Oct. 25, 2009
17. F. Sahlin, R. Larsson, A. Almqvist, and P. Lugt, "A Mixed Lubrication Model Incorporating Measured Surface Topography, Part 2: Roughness Treatment, Model Validation, and Simulation," *ARCHIVE Proceedings of the Institution of Mechanical Engineers Part J Journal of Engineering Tribology*, Vol. 224, No. 4, pp. 353-365, 2009
18. P. Yang and S. Wen, "A Generalized Reynolds Equation for Non-Newtonian Thermal Elastohydrodynamio Lubrication," *Journal of Tribology*, Vol. 112, No. 4, pp. 631-636, 2008
19. N. Ren, D. Zhu, and W. Chen, "A Three-Dimensional Deterministic Model for Rough Surface Line-Contact EHL Problems," *Journal of Tribology*, Vol. 131, No. 1, pp. 011501-011509, 2008
20. X. Ai, "Numerical Analyses of Elastohydrodynamically Lubricated Line and Point Contacts with Rough Surfaces by using Semi-System and Multigrid Methods," Evanston, Northwestern University, 1993